ORIGINAL SCIENTIFIC PAPER OPEN ACCESS

Biomechanical analysis of impact static loading on dental resin composites using homotopy perturbation

Olurotimi A. Adeleye[1*], Boluwaji Omokagbo[1], Gbeminiyi Sobamowo[2]

[1] University of Lagos, Biomedical Engineering Department, Akoka, Lagos, Nigeria

[2] University of Lagos, Mechanical Engineering Department, Akoka, Lagos, Nigeria

ARTICLE INFO

[*] **Correspondence:** oadeleye@unilag.edu.ng

DOI:

UDC: 621(497.11) **ISSN:** 2812-9474

Article history: Received 22 August 2024; Revised 26 September 2024; Accepted 4 October 2024

ABSTRACT

The biomechanical analysis of the impact static loading on dental resin composites (DRC) using homotopy perturbation method is here presented. The DRC are commonly used to restore damaged teeth due to their aesthetic of appeal and biocompatibility. However, their strain rate dependent response under different loading conditions still remains a subject of interest and research. Consequently, the present study provides analytical solutions to the developed predictive nonlinear ordinary differential equation mathematical model for the strain rate viscoelastic deformation behaviors of DRC under impact static loading. The solution of the developed governing model was obtained by applying the Homotopy Perturbation Method (HPM). The obtained analytical solution was validated with the Runge-Kutta Order four (RK4) numerical method and good agreement was established between them. The effects of material applied stress, viscosity, stiffness, and initial strain on the model were investigated. It is observed from the study that when an applied impact static stress was applied on the material model, there was no conventional decrease in strain before the progressive increase until it reaches relaxation. Secondly, as the stiffness parameter increases, the time to reach relaxation also increases. In addition, as the viscosity increases, the material resistance to deformation also increases. And as the initial strain increases, there was increase in the time to reach the relaxation point and increase in the relaxation values. This study provides a guide for the development of improved dental composites and restoration techniques. The study also provides an insight for advancements in restorative dentistry and lead to enhanced clinical outcomes for patients. It is envisaged that this present study will serve as yardstick for subsequent works in the research area.

KEYWORDS

Dental implants, Viscoelastic model, Impact loading; Homotopy perturbation method.

1. INTRODUCTION

The application of composites and polymers in several areas of use has advanced appreciably over past decades. However, despite their better properties, their application in crucial load carrying members is still restricted. A very important reason out of many considered to be responsible for the limited application of the materials is the challenges with developing reliable predictive models for the material deformation [1]. Majority of the polymer-based biomaterials exhibits time dependent linear deformation, but at elevated temperature and stress, and continuous loading, the deformation can no longer be described with the linear deformation model. The formation of polymeric composites is a heterogeneous structure with distinct constituent and geometric properties. This heterogeneous

structure of the composites which is motivated by the dissimilar properties of the compositions and different types of the arrangements of the microstructure creates the complexity in the prediction of the time-dependent deformation of the material [2,3].

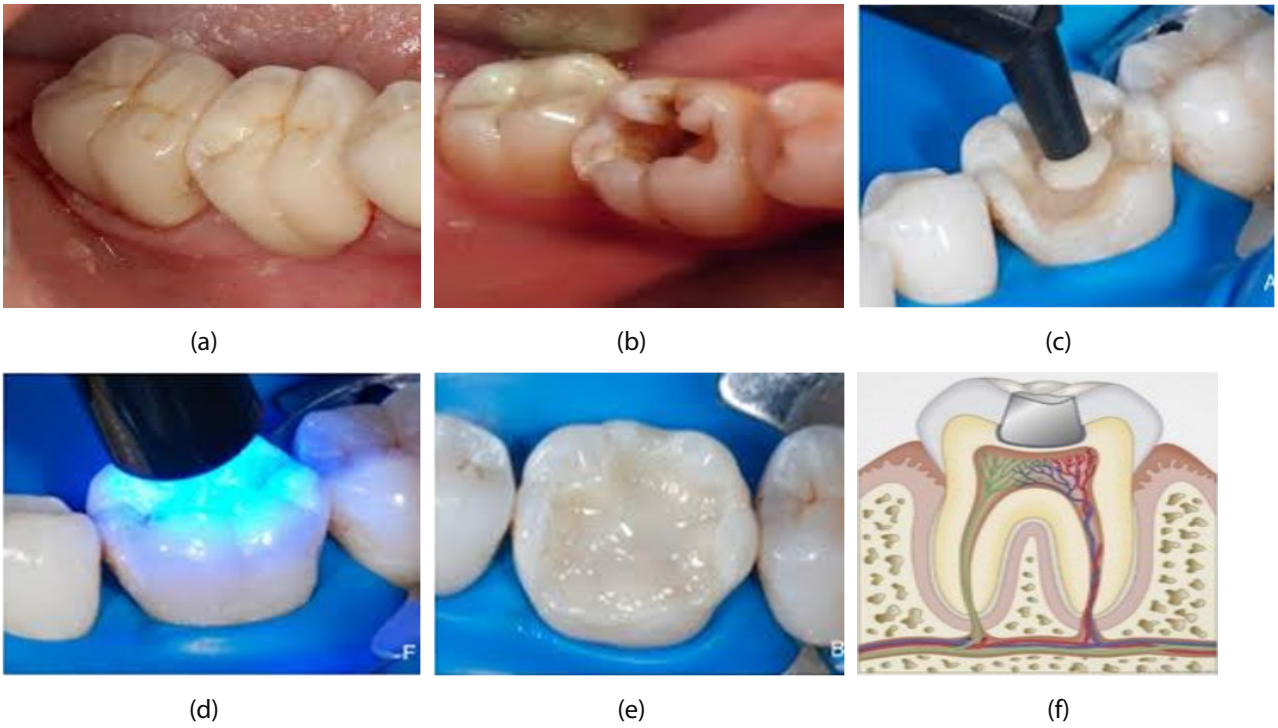

(a) (b) (c)

(d) (e) (f)

Figure 1: (a) Normal tooth, (b) Decay tooth, (c) Process of decay tooth restoration, (d) Dental resin composite Curing light, (e) Restored tooth with dental resin composite, (f) Schematic of cured dental resin composite

The dental resins composites materials have wide applications in restorative dentistry. The composites can be applied to the denture without taking out the healthy tissues of the tooth. The bonding ability of the dental resin composites has also made it useful for adjustment of the occlusion, repairs of injured or diseased anterior and posterior teeth, bonding of brackets for orthodontics, application and cementation of the restorative material (Figure 1(a)–(f)), and the total transformation of aesthetic teeth. For this reason, the application of the material has increased in conservative and modern dentistry [4]. In a recent study of the deformation behavior of a human dentin under uniaxial compression loading with size and rate effects, it is shown that the dentin is an elastic and mechanically isotropic strong hard tissue, which exhibits plasticity and crack growth suppress ability [5,6].

Quite a number of studies have been done to investigate the deformation of the biomaterials used for the denture and some of them have been done for the mathematical models of these deformation behavior. But only a few studies have been carried out in the past recent studies on the mathematical models for the description of the dental resin composites deformation behavior. One of such models is the viscohypoelastic used for describing the shrinkage behavior in the dental resin composite [7]. In the study, a viscoelastic time continuous function in the Maxwell model and the Young's modulus were used in the governing model. In another study, the viscoplastic model with an application of the Finite Element Method was applied for the shrinkage deformation from the curing of dental resin composites [8]. The COMSOL Multiphysics software was applied for implementing a cure-temperature-time model for a viscoelastic model [9]. In order to implement the base equations in the software, they were modified. The deformation of DRC as a result of curing shrinkage has been shown to be nonlinear and time dependent [10]. Therefore, the viscoelastic model can be used to predict the deformation behavior of the DRC.

Studies have shown that the polymeric biomaterials have high inclination towards nonlinear behavior [11], which have been represented by linear models [12, 13]. These linear models have not adequately captured the observed the time-dependent deformation in DRC biomaterials [14]. Attempts have been made to capture the nonlinearities and model them appropriately [11, 15]. The effects of chemical properties such as acids, water, etc., have also been considered on biomaterials [16], even though this effect seemed insignificant because of small quantity of chemicals used in the biomaterial under study. This means that the effects depend on the percentage of the chemical compositions. The viscoelastic model is a function of the material elasticity, viscosity, and Young's modulus, and it is time and path dependent [17,18]. It is evident that the biomaterial deformation behavior depends majorly on its mechanical properties [19]. Such properties include ductility, softness, (or hardness), stiffness, which are considered while developing predictive models for the deformation behavior of a material [20]. The loading conditions of these biomaterials also affects the deformation behavior or their strain rate dependent response which remain a subject of

interest and research. Consequently, in the present study, a predictive nonlinear ordinary differential equation mathematical model for the strain rate viscoelastic deformation behaviors of DRC under impact static loading has been developed.

The developed governing model in the present study a nonlinear differential equation with solutions that cannot be obtained with the existing traditional analytical methods. A special analytical method for strongly nonlinear ordinary differential equation known as the Homotopy Perturbation Method is applied in this present study. The technique was originally developed by Ji-Huan He [21] for providing solutions for linear and nonlinear integral and differential equations. The method is a powerful analytical technique which needs no approximation. The effectiveness of the method has been demonstrated in some few recent studies. One of such is its comparison with the results obtained with the Adomian Decomposition Method (ADM) for solving nonlinear problems. [22]. The HPM has been applied to obtain solutions for nonlinear oscillators [23] and high level of accuracy was observed. The study has notably shown how effective and accurate it can be over the ADM. The HPM and the Homotopy Analysis Method (HAM) have been applied to solve the generalized Zakharov equations [24] and the absolute errors are very minimal. The technique was also applied in the study of heat transfer in longitudinal fins where its effectiveness was demonstrated [25]. The HPM has been applied to solve hyperbolic partial differential equation [26], and the results show good accuracy and effectiveness. The HPM and the Collocation method (CM) were applied to study the thermal performance of porous fin with temperature-dependent heat generation [27] and the accuracy of the HPM was established. The HPM has also been combined with Laplace method to solve the Lane – Emden type of differential equations [28]. In the study of heat transfer analysis of non-Newtonian natural convective fluid flow, the results obtained with HPM was compared with that of the Daftardar-Gejiji and Jafari methods [29] and the HPM was again shown to be effective in its application and also when further compared with the RK4 Numerical method.

Hence, the main objective of this current study is to develop a nonlinear ordinary differential equation governing model for the impact static loading of dental resin composite implants and to determine the analytical solutions with the Homotopy Perturbation Method. In order to validate the obtained solutions of the problem by the HPM, the Runge-Kutta Order four (RK4) method are applied to solve the same problem. The solutions are also compared with obtained results from past studies. The effects of material applied stress, viscosity, stiffness, and initial strain on the governing model are then investigated.

2. MODEL FORMULATION FOR IMPLANT DEFORMATION UNDER IMPACT STATIC LOADING

Consider the schematic of a specimen of dental composite carrying static load as depicted in Figure 2.

(a)

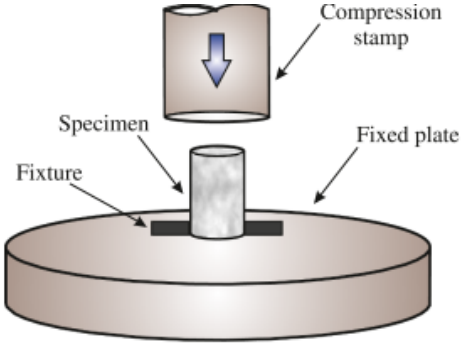

(b)

The compressive strength of the dental specimen may be calculated from:

$$S = \frac{P}{A_\phi} \tag{1}$$

Since the cross section of the specimen under investigation is idealized to be circular, then:

$$A_\phi = \frac{\pi D^2}{4} \tag{2}$$

Substituting Eq. (2) into Eq. (1), the compressive strength of the dental composite under static loading is obtained as;

$$S = \frac{4P}{\pi D^2} \tag{3}$$

Similarly, the strain incurred to get to the magnitude may be obtained from;

$$\varepsilon = \frac{\delta}{L} = \frac{4P}{E\pi D^2} \tag{4}$$

The unidirectional thermal stress due to the change in temperature experienced by this dental specimen during static loading may be obtained by comparing its elastic property with its flexural property. The change in dimension experienced due to change in temperature is:

$$\delta = \alpha L \Delta\theta \tag{5}$$

Also, from Eq. (4),

$$\delta = \frac{4PL}{E\pi D^2} = \frac{PL}{AE} = \sigma_\theta \left(\frac{L}{E}\right) \tag{6}$$

Equating Eq. (5) and Eq. (6),

$$\delta = \alpha L \Delta\theta = \sigma_\theta \left(\frac{L}{E}\right) \tag{7}$$

Which on simplifying gives the thermal stress as:

$$\sigma_\theta = E\alpha\Delta\theta \tag{8}$$

$$\frac{d\varepsilon(t)}{dt} + \frac{c}{L}\varepsilon_e(t) = 0 \tag{9}$$

$$\varepsilon(t) = -\frac{c}{L}\int_0^t \varepsilon_e(t)dt \tag{10}$$

$$\sigma(t) = \frac{EA_b}{A_s}\varepsilon_t(t) \tag{11}$$

3. MODEL FORMULATION FOR CREEP STRAIN IN DENTAL COMPOSITE

Consider the schematic creep deformation and correction as depicted in Figure (3.3). Using Bauer's theory (1984), loading force function $\phi(\varepsilon)$ can be expressed as:

$$\ddot{\varepsilon}\frac{d\phi}{d\varepsilon} + \dot{\varepsilon}^2\frac{d^2\phi}{\partial\varepsilon^2} + \frac{b}{c}\dot{\varepsilon}\frac{d\phi}{d\varepsilon} + \frac{a}{c}\phi = \frac{\sigma}{c} \tag{12}$$

The model uses a logarithmic force law given as;

$$\phi(\varepsilon) = \log_e\left(\varepsilon_0 - \frac{\varepsilon}{\varepsilon_0}\right) \tag{13}$$

Using Eq. (13) in Eq. (12), we have:

$$-c\frac{\ddot{\varepsilon}\left(\varepsilon_0^2 - \varepsilon\right) + \dot{\varepsilon}^2}{\left(\varepsilon_0^2 - \varepsilon\right)^2} - b\frac{\dot{\varepsilon}}{\left(\varepsilon_0^2 - \varepsilon\right)} + a\log_e\left(\varepsilon_0 - \frac{\varepsilon}{\varepsilon_0}\right) = \sigma\begin{cases}0 & \textit{Free}\\ \sigma & \textit{Static loading}\end{cases} \tag{14}$$

This equation will be used to obtain the creep deformation of the composite under impact static loading.

To establish the novelty of the work, it is important to state that previous studies considered similar model with the applied stress, σ= 0. This present study will consider the case of σ≠0 and obtain the creep deformation for the dental composite under impact static loading.

Analytical method will also be used to obtain the deformation of the system and for model validation. Consequently, recall the evolution deformation equation as:

$$-c\frac{\ddot{\varepsilon}\left(\varepsilon_0^2 - \varepsilon\right) + \dot{\varepsilon}^2}{\left(\varepsilon_0^2 - \varepsilon\right)^2} - b\frac{\dot{\varepsilon}}{\left(\varepsilon_0^2 - \varepsilon\right)} + a\log_e\left(\varepsilon_0 - \frac{\varepsilon}{\varepsilon_0}\right) = \sigma \tag{15}$$

To obtain the dynamic behaviour of the dental composite, a strain-displacement function using variable change was introduced as:

$$e^{\xi} = \frac{\varepsilon_0^2 - \varepsilon}{\varepsilon_0} \tag{16}$$

Where

$$\omega_o = \frac{b}{c}, \quad \lambda = \frac{a}{c}, \quad \alpha = \frac{k}{c}, \quad \text{and} \quad x = \ln\left(\varepsilon_0 - \frac{\varepsilon}{\varepsilon_0}\right) \tag{17}$$

Simplifying Equation (15) and substituting Equation (16) gives the following nonlinear model;

$$\ddot{x} + (\omega_o - 1)\dot{x} + \dot{x}\,\dot{x}^2 + x(\lambda - \alpha) - \alpha = 0 \tag{18}$$

4. METHOD OF SOLUTION: HOMOTOPY PERTURBATION METHOD (HPM)

Equation (18) is a nonlinear differential equation which is to be solved using HPM. To apply HPM, consider a given arbitrary function $f(r)$

$$L(u) + N(u) = f(r), \; r \in \Omega \tag{19}$$

With the following boundary conditions:

$$B\left(u, \frac{\partial u}{\partial n}\right) = 0, \; r \in \Gamma \tag{20}$$

Where $f(r)$ is a known analytical function, $L(u)$ and $N(u)$ are linear and nonlinear operators respectively, and Γ is a boundary in a domain Ω.

The Homotopy Perturbation Method proposed by Ji-Huan He [11], is expressed as:

$$H(u,p) = (1-p)[L(u) - L(u_0)] + p[L(u) + N(u) - f(r)] = 0 \tag{21}$$

Where p is an embedding parameter and u_0 is an initial approximation of Eqn (18).

The solution can be obtained as:

$$x = x_0 + px_1 + p^2x_2 + p^3x_3 + p^4x_4 + p^5x_5 \ldots \tag{22}$$

$$H(x,p) = (1-p)\left(\frac{d^2x}{dt^2} - \frac{d^2x_0}{dt^2}\right) + p\left(\frac{d^2x}{dt^2} + (\omega_o - 1)\frac{dx}{dt} + \frac{dx}{dt}\left(\frac{dx}{dt}\right)^2 + (\lambda - \alpha)x - \alpha\right) = 0 \tag{23}$$

Substitute equation (22) into (23)

$$\begin{aligned}
&(1-p)\left(\frac{d^2\left(x_0 + p^1x_1 + p^2x_2 + p^3x_3 + p^4x_4 + p^5x_5\right)}{dt^2}\right) + p\left(\frac{d^2\left(x_0 + p^1x_1 + p^2x_2 + p^3x_3 + p^4x_4 + p^5x_5\right)}{dt^2}\right) \\
&+(w_0 - 1)\left(\frac{d\left(x_0 + p^1x_1 + p^2x_2 + p^3x_3 + p^4x_4 + p^5x_5\right)}{dt}\right) + \left(\frac{d\left(x_0 + p^1x_1 + p^2x_2 + p^3x_3 + p^4x_4 + p^5x_5\right)}{dt}\right) \\
&\left(\frac{d\left(x_0 + p^1x_1 + p^2x_2 + p^3x_3 + p^4x_4 + p^5x_5\right)}{dt}\right)^2 + \left(\lambda - \alpha\right)\left(x_0 + p^1x_1 + p^2x_2 + p^3x_3 + p^4x_4 + p^5x_5\right) - \alpha = o
\end{aligned} \tag{24}$$

When the coefficients of p^0, p^1, p^2, p^3, p^4, and p^5 are equated to zero, the solutions for x_0, x_1, x_2, x_3, x_4, and x_5 are then obtained. Expanding and resolving Eqn. (24) the coefficients of p^0, p^1, p^2, p^3, p^4, and p^5 are obtained as:

$$p^0\left[\frac{d^2x_o}{dt^2}\right] = 0 \tag{25}$$

$$p^1\left[\frac{d^2x_1}{dt^2}+(w_0-1)\frac{dx_o}{dt}+\frac{dx_o}{dt}\frac{dx_o}{dt}x_0+(\lambda-\alpha)x_0-\alpha\right]=0 \tag{26}$$

$$p^2\left[\begin{array}{l}\frac{d^2x_2}{dt^2}+(w_0-1)\frac{dx_1}{dt}+\frac{dx_0}{dt}\frac{dx_o}{dt}x_1+\frac{dx_0}{dt}\frac{dx_1}{dt}x_0\\+\frac{dx_1}{dt}\frac{dx_0}{dt}x_0+(\lambda-\alpha)x_1\end{array}\right]=0 \tag{27}$$

$$p^3\left[\begin{array}{l}\frac{d^2x_3}{dt^2}+(w_0-1)\frac{dx_2}{dt}+\frac{dx_0}{dt}\frac{dx_o}{dt}x_2+\frac{dx_0}{dt}\frac{dx_1}{dt}x_1\\+\frac{dx_1}{dt}\frac{dx_0}{dt}x_1+\frac{dx_0}{dt}\frac{dx_2}{dt}x_0+\frac{dx_1}{dt}\frac{dx_1}{dt}x_0\frac{dx_2}{dt}\frac{dx_0}{dt}x_0+(\lambda-\alpha)x_2\end{array}\right]=0 \tag{28}$$

$$p^4\left[\begin{array}{l}\frac{d^2x_4}{dt^2}+(w_0-1)\frac{dx_3}{dt}+\frac{dx_0}{dt}\frac{dx_0}{dt}x_3+\frac{dx_0}{dt}\frac{dx_1}{dt}x_2+\frac{dx_0}{dt}\frac{dx_2}{dt}x_1+\frac{dx_0}{dt}\frac{dx_3}{dt}x_0\\+\frac{dx_1}{dt}\frac{dx_0}{dt}x_2+\frac{dx_1}{dt}\frac{dx_1}{dt}x_1+\frac{dx_1}{dt}\frac{dx_2}{dt}x_0+\frac{dx_2}{dt}\frac{dx_0}{dt}x_1+\frac{dx_2}{dt}\frac{dx_1}{dt}x_0\\+\frac{dx_3}{dt}\frac{dx_0}{dt}x_0+(\lambda-\alpha)x_3\end{array}\right]=0 \tag{29}$$

$$p^5\left[\begin{array}{l}\frac{d^2x_5}{dt^2}+(w_0-1)\frac{dx_4}{dt}+\frac{dx_0}{dt}\frac{dx_0}{dt}x_4+\frac{dx_0}{dt}\frac{dx_1}{dt}x_3+\frac{dx_0}{dt}\frac{dx_2}{dt}x_2+\frac{dx_0}{dt}\frac{dx_3}{dt}x_1\\+\frac{dx_0}{dt}\frac{dx_4}{dt}x_0+\frac{dx_0}{dt}\frac{dx_1}{dt}x_2+\frac{dx_1}{dt}\frac{dx_0}{dt}x_3+\frac{dx_1}{dt}\frac{dx_1}{dt}x_2+\frac{dx_1}{dt}\frac{dx_2}{dt}x_1+\frac{dx_1}{dt}\frac{dx_3}{dt}x_2\\+\frac{dx_0}{dt}\frac{dx_2}{dt}x_1+\frac{dx_2}{dt}\frac{dx_0}{dt}x_2+\frac{dx_2}{dt}\frac{dx_1}{dt}x_1+\frac{dx_2}{dt}\frac{dx_2}{dt}x_0+\frac{dx_3}{dt}\frac{dx_0}{dt}x_1+\frac{dx_3}{dt}\frac{dx_1}{dt}x_0\\+\frac{dx_3}{dt}\frac{dx_1}{dt}x_0+(\lambda-\alpha)x_4\end{array}\right]=0 \tag{30}$$

With the following initial conditions;

$$\mathrm{x}_0(0)=\mathrm{x}_1(0)=\ldots\mathrm{x}_n(0)=0 \tag{31}$$

Using Eqns. (25-30), and the initial conditions in (31), the solutions for $x_0, x_1, x_2, x_3, x_4,$ and x_5 are obtained

$$x_0[t]=Log\left[\epsilon_o-\frac{\epsilon_1}{\epsilon_o}\right] \tag{32}$$

$$x_1[t]=\frac{1}{2}\left(t^2\alpha+t^2\alpha Log\left[-\frac{\epsilon_1}{\epsilon_o}+\epsilon_o\right]-t^2\lambda Log\left[-\frac{\epsilon_1}{\epsilon_o}+\epsilon_o\right]\right) \tag{33}$$

$$x_2[t]=\frac{1}{24}t^3\left(4-4\omega_o+t\alpha-t\lambda\right)\left(\alpha+\alpha Log\left[-\frac{\epsilon_1}{\epsilon_o}+\epsilon_o\right]-\lambda Log\left[-\frac{\epsilon_1}{\epsilon_o}+\epsilon_o\right]\right) \tag{34}$$

$$\begin{array}{l}x_3[t]=\frac{1}{720}\left(\alpha+\alpha Log\left[-\frac{\epsilon_1}{\epsilon_o}+\epsilon_o\right]-\lambda Log\left[-\frac{\epsilon_1}{\epsilon_o}+\epsilon_o\right]\right)\\\left(\begin{array}{l}30t^4-60t^4\omega_o+30t^4{\omega_o}^2+12t^5\alpha-12t^5\omega_o\alpha+t^6\alpha^2-12t^5\lambda+12t^5\omega_o\lambda-2t^6\alpha\lambda+t^6\lambda^2-\\60t^4\alpha Log\left[-\frac{\epsilon_1}{\epsilon_o}+\epsilon_o\right]-60t^4\alpha Log\left[-\frac{\epsilon_1}{\epsilon_o}+\epsilon_o\right]^2+60t^4\lambda Log\left[-\frac{\epsilon_1}{\epsilon_o}+\epsilon_o\right]^2\end{array}\right)\end{array} \tag{35}$$

$$x_4[t]=\frac{1}{40320}\left(\alpha+\alpha Log\left[-\frac{\epsilon_1}{\epsilon_o}+\epsilon_o\right]-\lambda Log\left[-\frac{\epsilon_1}{\epsilon_o}+\epsilon_o\right]\right)$$

$$\left(\begin{array}{l}
336t^5-1008t^5\omega_o+1008t^5\omega_o{}^2-336t^5\omega_o{}^3+168t^6\alpha+336t^6\omega_o\alpha\\
168t^6\omega_o{}^2\alpha-672t^6\alpha^2+24t^7\alpha^2-24t^7\omega_o\alpha^2+t^8\alpha^3-168t^6\lambda+336t^6\omega_o\lambda\\
-168t^6\omega_o{}^2\lambda-48t^7\alpha\lambda+48t^7\omega_o\alpha\lambda-3t^8\alpha^2\lambda+24t^7\lambda^2-24t^7\omega_o\lambda^2\\
+3t^8\alpha\lambda^2-t^8\lambda^3-2688t^7\alpha Log\left[-\frac{\epsilon_1}{\epsilon_o}+\epsilon_o\right]+2688t^5\omega_o\alpha Log\left[-\frac{\epsilon_1}{\epsilon_o}+\epsilon_o\right]\\
-1904t^6\alpha^2 Log\left[-\frac{\epsilon_1}{\epsilon_o}+\epsilon_o\right]+1904t^6\alpha\lambda Log\left[-\frac{\epsilon_1}{\epsilon_o}+\epsilon_o\right]-2688t^5\alpha Log\left[-\frac{\epsilon_1}{\epsilon_o}+\epsilon_o\right]^2\\
+2688t^5\omega_o\alpha Log\left[-\frac{\epsilon_1}{\epsilon_o}+\epsilon_o\right]^2-1232t^6\alpha^2 Log\left[-\frac{\epsilon_1}{\epsilon_o}+\epsilon_o\right]^2+2688t^5\lambda Log\left[-\frac{\epsilon_1}{\epsilon_o}+\epsilon_o\right]^2\\
+2688t^5\omega_o\lambda Log\left[-\frac{\epsilon_1}{\epsilon_o}+\epsilon_o\right]^2+2464t^6\alpha\lambda Log\left[-\frac{\epsilon_1}{\epsilon_o}+\epsilon_o\right]^2\\
-1232t^6\lambda^2 Log\left[-\frac{\epsilon_1}{\epsilon_o}+\epsilon_o\right]^2
\end{array}\right) \tag{36}$$

$$x_5[t]=\frac{1}{3628800}\left(\alpha+\alpha Log\left[-\frac{\epsilon_1}{\epsilon_o}+\epsilon_o\right]-\lambda Log\left[-\frac{\epsilon_1}{\epsilon_o}+\epsilon_o\right]\right)$$

$$\left(\begin{array}{l}
5040t^6-20160t^6\omega_o+30240t^6\omega_o{}^2-20160t^6\omega_o{}^3+5040t^6\omega_o{}^4+2880t^7\alpha\\
-8640t^7\omega_o\alpha+8640t^7\omega_o{}^2\alpha-2880t^7\omega_o{}^3\alpha-66240t^7\alpha^2+540t^8\alpha^2+66240t^7\omega_o\alpha^2\\
-1080t^8\omega_o\alpha^2+540t^8\omega_o{}^2\alpha^2-14580t^8\alpha^3+40t^9\alpha^3-40t^9\omega_o\alpha^3+t^{10}\alpha^4-2880t^7\lambda\\
+8640t^7\omega_o\lambda-8640t^7\omega_o{}^2\lambda+2880t^7\omega_o{}^3\lambda-1080t^8\alpha\lambda+2160t^8\omega_o\alpha\lambda-1080t^8\omega_o{}^2\alpha\lambda\\
+14580t^8\alpha^2\lambda-120t^9\alpha^2\lambda+120t^9\omega_o\alpha^2\lambda-4t^{10}\alpha^3\lambda+540t^9\lambda^2-1080t^8\omega_o\lambda^2\\
+540t^9\omega_o{}^2\lambda^2+120t^9\alpha\lambda^2-120t^9\omega_o\alpha\lambda^2+6t^{10}\alpha^2\lambda^2-40t^9\lambda^3+40t^9\omega_o\lambda^3-4t^{10}\alpha\lambda^3\\
+t^{10}\lambda^4-110880t^6\alpha Log\left[-\frac{\epsilon_1}{\epsilon_o}+\epsilon_o\right]+221760t^6\omega_o\alpha Log\left[-\frac{\epsilon_1}{\epsilon_o}+\epsilon_o\right]\\
-110880t^6\omega_o{}^2\alpha Log\left[-\frac{\epsilon_1}{\epsilon_o}+\epsilon_o\right]-174240t^7\alpha^2 Log\left[-\frac{\epsilon_1}{\epsilon_o}+\epsilon_o\right]\\
+174240t^7\omega_o\alpha^2 Log\left[-\frac{\epsilon_1}{\epsilon_o}+\epsilon_o\right]-32940t^8\alpha^3 Log\left[-\frac{\epsilon_1}{\epsilon_o}+\epsilon_o\right]\\
+174240t^7\alpha\lambda Log\left[-\frac{\epsilon_1}{\epsilon_o}+\epsilon_o\right]-174240t^7\omega_o\alpha\lambda Log\left[-\frac{\epsilon_1}{\epsilon_o}+\epsilon_o\right]\\
+65880t^8\alpha^2\lambda Log\left[-\frac{\epsilon_1}{\epsilon_o}+\epsilon_o\right]-32940t^8\alpha\lambda^2 Log\left[-\frac{\epsilon_1}{\epsilon_o}+\epsilon_o\right]\\
-110880t^6\alpha Log\left[-\frac{\epsilon_1}{\epsilon_o}+\epsilon_o\right]^2+221760t^6\omega_o\alpha\lambda Log\left[-\frac{\epsilon_1}{\epsilon_o}+\epsilon_o\right]^2\\
-110880t^6\omega_o{}^2\alpha Log\left[-\frac{\epsilon_1}{\epsilon_o}+\epsilon_o\right]^2+80640t^6\alpha^2 Log\left[-\frac{\epsilon_1}{\epsilon_o}+\epsilon_o\right]^2\\
-108000t^7\alpha^2 Log\left[-\frac{\epsilon_1}{\epsilon_o}+\epsilon_o\right]^2+108000t^7\omega_o\alpha^2 Log\left[-\frac{\epsilon_1}{\epsilon_o}+\epsilon_o\right]^2\\
-18360t^8\alpha^2 Log\left[-\frac{\epsilon_1}{\epsilon_o}+\epsilon_o\right]^2+110880t^6\lambda Log\left[-\frac{\epsilon_1}{\epsilon_o}+\epsilon_o\right]^2\\
-221760t^6\omega_o\lambda Log\left[-\frac{\epsilon_1}{\epsilon_o}+\epsilon_o\right]^2+11880t^6\omega_o{}^2\lambda Log\left[-\frac{\epsilon_1}{\epsilon_o}+\epsilon_o\right]^2\\
+216000t^7\alpha\lambda Log\left[-\frac{\epsilon_1}{\epsilon_o}+\epsilon_o\right]^2-216000t^7\omega_o\alpha\lambda Log\left[-\frac{\epsilon_1}{\epsilon_o}+\epsilon_o\right]^2\\
+55080t^8\alpha^2\lambda Log\left[-\frac{\epsilon_1}{\epsilon_o}+\epsilon_o\right]^2-108000t^7\lambda^2 Log\left[-\frac{\epsilon_1}{\epsilon_o}+\epsilon_o\right]^2\\
+108000t^7\omega_o\lambda^2 Log\left[-\frac{\epsilon_1}{\epsilon_o}+\epsilon_o\right]^2-55080t^8\alpha\lambda^2 Log\left[-\frac{\epsilon_1}{\epsilon_o}+\epsilon_o\right]^2
\end{array}\right)$$

$$\left(\begin{array}{l} +18360t^8\lambda^3 Log\left[-\frac{\epsilon_1}{\epsilon_o}+\epsilon_o\right]^2+161280t^6\alpha^2 Log\left[-\frac{\epsilon_1}{\epsilon_o}+\epsilon_o\right]^3 \\ -161280t^6\alpha\lambda Log\left[-\frac{\epsilon_1}{\epsilon_o}+\epsilon_o\right]^3+80640t^6\alpha^2 Log\left[-\frac{\epsilon_1}{\epsilon_o}+\epsilon_o\right]^4 \\ -161280t^6\alpha\lambda Log\left[-\frac{\epsilon_1}{\epsilon_o}+\epsilon_o\right]^4+80640t^6\lambda^2 Log\left[-\frac{\epsilon_1}{\epsilon_o}+\epsilon_o\right]^4 \end{array}\right) \tag{37}$$

Since

$$X[t]=x_0[t]+x_1[t]+x_2[t]+x_3[t]+x_4[t]+x_5[t] \tag{38}$$

The strain equation $\varepsilon(t)$ can be expressed from Eqn. (16) as

$$\varepsilon(t)=\varepsilon_0^2-\varepsilon_0 e^x \tag{39}$$

Using ε_0=1,

$$\varepsilon(t)=1-e^x \tag{40}$$

And substituting Eqn. (38) into (40), the strain equation is expressed as

$$\varepsilon(t)=1-Exp\left[X(t)\right] \tag{41}$$

5. RESULTS AND DISCUSSION

The results obtained from applying Homotopy Perturbation Method for the biomechanical analysis of the problem of impact loading of dental resin composites are presented in Table 1. The Runge-Kutta Order four (RK4) is then applied to obtain solutions to the problem of impact loading of dental resin composites in order to validate the same results obtained with the HPM. Both results from the HPM and RK4 are presented and compared in Table 1. From the results, minimal errors of less than 5% are observed in the obtained solutions and good agreement is achieved between the HPM analytical method and the RK4 numerical method.

Table 1. Comparison of HPM and Numerical Method results

The results of HPM, DTM and Numerical methods for $\varepsilon(t)$ *for* $\varepsilon_0 = 1, \varepsilon_i = 0.9, \lambda = 2, \omega_0 = 0.5, \sigma = 0$

t	HPM	DTM	NUM	Error o HPM	Error of DTM
0.00	0.90000	0.90000	0.90000	0.00000	0.00000
0.05	0.89979	0.89993	0.89986	-0.00007	0.00007
0.10	0.89918	0.89973	0.89946	-0.00029	0.00027
0.15	0.89814	0.89941	0.89882	-0.00068	0.00059
0.20	0.89668	0.89898	0.89795	-0.00127	0.00103
0.25	0.89479	0.89845	0.89687	-0.00208	0.00158
0.30	0.89244	0.89783	0.89559	-0.00315	0.00224
0.35	0.88964	0.89712	0.89412	-0.00448	0.00299
0.40	0.88636	0.89633	0.89248	-0.00612	0.00385
0.45	0.88262	0.89546	0.89066	-0.00804	0.00481
0.50	0.87841	0.89453	0.88867	-0.01026	0.00587
0.55	0.87376	0.89355	0.88652	-0.01276	0.00703
0.60	0.86873	0.89251	0.88422	-0.01549	0.00830
0.65	0.86339	0.89145	0.88176	-0.01837	0.00969
0.70	0.85786	0.89037	0.87915	-0.02129	0.01122
0.75	0.85231	0.88931	0.87641	-0.02410	0.01291
0.80	0.84698	0.88830	0.87352	-0.02654	0.01478
0.85	0.84215	0.88739	0.87049	-0.02835	0.01690
0.90	0.83818	0.88663	0.86733	-0.02915	0.01930
0.95	0.83552	0.88612	0.86404	-0.02852	0.02208
1.00	0.83463	0.88594	0.86062	-0.02600	0.02531

The response of the material to an initial strain 0.9 is shown in Fig. 4. The material model is such that the material increases in strain rate at applied strain of 0.9. When the applied strain is more than ε_0^2, there is an increase in the material deformation. Otherwise, the initial strain should be kept lower or made equal with ε_0^2. The decrease in the ratio of the material viscosity λ results in increase in the inertial which shows an increase in resistance to deformation. But when the material viscosity is increased, the inertial property decreases. Similarly, when the material stiffness ω_0 is increased, there is a decrease in the inertial property of the material and a decrease in the material stiffness results in an increase in the inertial.

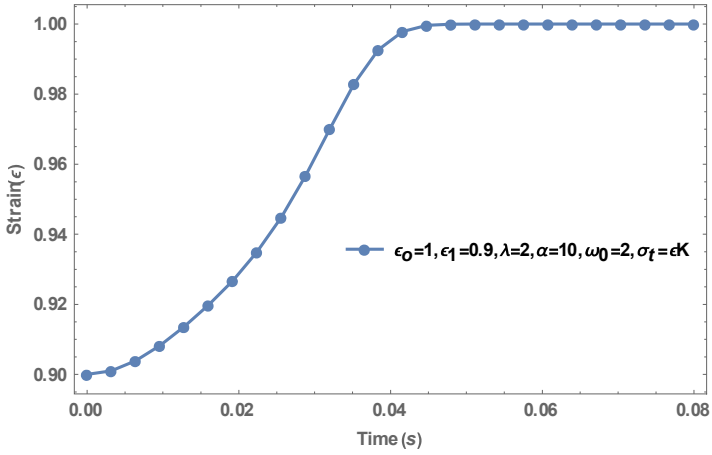

Figure 4: Deformation behavior of material with specified material parameters $\varepsilon_0 = 1, \varepsilon_1 = 0.9, \lambda = 2, \alpha = 10, \omega_0 = 2$

The absence and the presence of the impact static loading $\sigma_t = 0$ and $\sigma_t = \varepsilon K$ are shown in Figure 5. In the absence of the impact static loading where $\sigma_t = 0$, the deformation of the material reduces to a minimum point from the initial strain before it gradually picks up until it reaches the relaxation point. But in the presence of the impact static loading, the material does not exhibit any decrease in deformation before it increases and shows relaxation. The effects of material viscosity on the material response when the stiffness $\omega_0 = 2$ to $\omega_0 = 8$ is shown in Fig. 6.

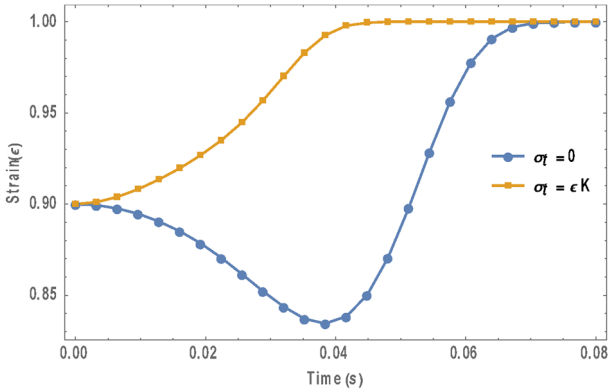

Figure 5: Comparison between the absence and presence of impact static loading $\varepsilon_0 = 1, \varepsilon_1 = 0.9, \lambda = 2, \alpha = 10, \omega_0 = 2$

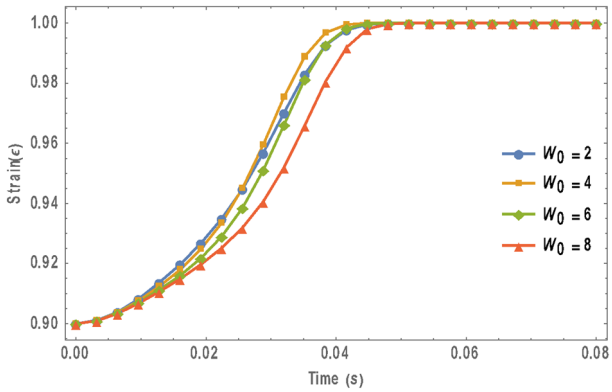

Figure 6: Effects of varying stiffness on material response $\varepsilon_0 = 1, \varepsilon_1 = 0.9, \alpha = 10, \lambda = 2$

It is observed that at different values of the stiffness parameter, there is no much difference in the rate at which the material reaches the relaxation point. The material reaches relaxation at the lowest value of the stiffness parameter faster than at the highest value of the stiffness parameter. It also shows that the material stiffness increases with increase in time. The response of the material at varying viscosity is presented in Fig. 7. Material viscosity generally influences its resistance to deformation and this is observed in the results in Fig. 7.

From the results, it is observed that when the viscosity increases, the material resistance to deformation increases. And when the viscosity decreases, there is a resulting decrease in material resistance to deformation. The material exhibits slight increase in strain for a short period before the relaxation sage. Furthermore, a increase in the viscosity results in an increase in strain and in the time period before it reaches the relaxation point.

In the investigation of the effects of varying initial strain in Figure 8, it is observed that the relaxation point is reached faster at lower initial strains than at higher initial strains and secondly the relaxation point is not constant as observed in other parameters, but varies. As the initial strain increases, a corresponding increase is observed in the relaxation values. The time in the relaxation region last longer with varying initial strain ε_0. When the applied strain is ε_i is farther from the initial strain ε_0, the deformation in the material reduces.

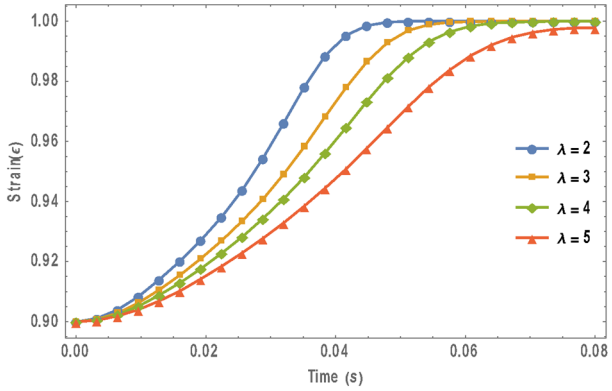

Figure 7: Effects of varying viscosity on material response $\varepsilon_0 = 1, \varepsilon_1 = 0.9, \alpha = 10, \omega_0 = 2$

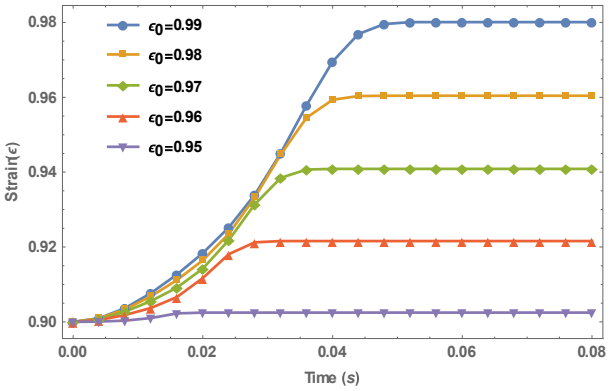

Figure 8: Effects of varying initial strain ε_0 on material response $\varepsilon_0 = 1, \alpha = 10, \omega_0 = 2, \lambda = 2$

The deformation behavior and strains as a result of applied stress is shown in Figure 9. The results shows that the material response is faster and reaches relaxation at high strains. At lower strains, the material takes longer time takes longer time before it reaches its relaxation point. Another observation is that the material does not reach the maximum relaxation value of 1 when the strain is lower than 0.85. this shows that the strain has great influence on the relaxation of the material deformation behavior.

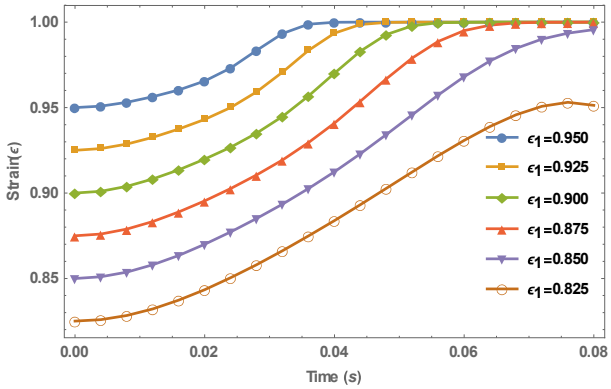

Figure 9: Effects of varying strain on material response $\varepsilon_0 = 1, \alpha = 10, \omega_0 = 2, \lambda = 2$

6. CONCLUSION

In this study, the biomechanical analysis of the impact static loading on dental resin composites (DRC) using homotopy perturbation method has been presented. The solutions of the developed nonlinear ordinary differential equation mathematical model for the strain rate viscoelastic deformation behaviors of DRC under impact static loading has been obtained using the homotopy perturbation method and validated with the numerical Runge-Kutta method of fourth order. From the study, it is observed that when an applied impact static stress was applied on the material model, there was no conventional decrease in strain before the progressive increase until it reaches relaxation. Secondly, as the stiffness parameter increases, the time to reach relaxation also increases. In addition, as the viscosity increases, the material resistance to deformation also increases. And as the initial strain increases, there was increase in the time to reach the relaxation point and increase in the relaxation values. This study provides a guide for the development of improved dental composites and restoration techniques. The study also provides an insight for advancements in restorative dentistry and lead to enhanced clinical outcomes for patients.

REFERENCES

[1] Y. Zhang, Z. Xia, and F. Ellyin, "Nonlinear viscoelastic micromechanical analysis of fibre-reinforced polymer laminates with damage evolution", International Journal of Solids and Structures, Vol. 42(2), pp. 591–604, https://doi.org/10.1016/j.ijsolstr.2004.06.02, (2005)

[2] J. S. Kim and A. H. Muliana, "A combined viscoelastic-viscoplastic behavior of particle reinforced composites", International Journal of Solids and Structures, Vol. 47(5), pp. 580–594, https://doi.org/10.1016/j.ijsolstr.2009.10.019, (2010)

[3] Y. Chen, X. Shi, Z. Zhao, Z. Guo, and Y. Li, "A thermo-viscoelastic model for particle-reinforced composites based on micromechanical modeling", Acta Mechanica Sinica, Vol. 37(3), pp. 402–413, https://doi.org/10.1007/s10409-020-01035-1, (2021)

[4] K. D. Jandt and B. W. Sigusch, "Future perspectives of resin-based dental materials", Dental Materials, Vol. 25(8), pp. 1001–1006, https://doi.org/10.1016/j.dental.2009.02.009, (2009)

[5] L. H. He and M. V. Swain, "Understanding the mechanical behaviour of human enamel from its structural and compositional characteristics", Journal of the Mechanical Behavior of Biomedical Materials, Vol. 1(1), pp. 18–29, https://doi.org/10.1016/j.jmbbm.2007.05.001, (2008)

[6] J. Andrejovská, O. Petruš, D. Medveď, M. Vojtko, M. Riznič, P. Kizek, and J.Dusza, "Hardness and indentation modulus of human enamel and dentin", Surface and Interface Analysis, Vol. 55(4), pp. 270–278, https://doi.org/10.1002/sia.7187, (2023)

[7] W. Gambin, "Visco-hypoelastic model of photo-polymerization process for small changes of temperature," Archives of Mechanics, Vol. 62(5), pp. 379–403, (2010)

[8] G. A. Laughlin, "Nonlinear finite element modeling of dental composite polymerization behavior", PhD. Thesis, University of Missouri (USA), (2003)

[9] B. Patham, "COMSOL® Implementation of a viscoelastic model with cure-temperature-time superposition for predicting cure stresses and springback in a thermoset resin", Proceedings of the COMSOL Conference, Bangalore (India), (2009)

[10] L. F. Pontes, E. B. Alves, B. P. Alves, R. Y. Ballester, C. G. B. T. Dias, C. M. Silva, "Mechanical properties of nanofilled and microhybrid composites cured by different light polymerization modes", General Dentistry, Vol. 61(3), p. 30-3, (2013)

[11] R. H. Ewoldt, A. E. Hosoi, and G. H. McKinley, "Nonlinear viscoelastic biomaterials: Meaningful characterization and engineering inspiration", Integrative and Comparative Biology, Vol. 49(1), pp. 40–50, Jul. 2009, https://doi.org/10.1093/icb/icp010, (2009)

[12] Z. G. Karaji, R. Hedayati, B. Pouran, I. Apachitei, and A.A. Zadpoor, "Effects of plasma electrolytic oxidation process on the mechanical properties of additively manufactured porous biomaterials", Materials Science and Engineering: C, Vol. 76: pp. 406-416, https://doi.org/10.1016/j.msec.2017.03.079, (2017)

[13] B. Basu, "Biomaterials for musculoskeletal regeneration", Indian Institute of Science, Bangalore (India), pp. 175-222, https://doi.org/10.1007/978-981-10-3059-8_6, (2017)

[14] A. W. Chan and R. J. Neufeld, "Modeling the controllable pH-responsive swelling and pore size of networked alginate based biomaterials", Biomaterials, Vol. 30(30), pp. 6119–6129, https://doi.org/10.1016/j.biomaterials.2009.07.034, (2009)

[15] M. D. Monsia, "A mathematical model for predicting the relaxation of creep strains in materials", Physical Review & Research International, Vol. 2(3), pp. 107-124, (2012)

[16] R. C. de Guzman, J. M. Saul, and M. D. Ellenburg, "Mechanical and biological properties of keratose biomaterials", Biomaterials, Vol. 32(32), pp. 8205-8217, https://doi.org/10.1016/j.biomaterials.2011.07.054, (2011)

[17] N. Weber, A. Pesnell, D. Bolikal, J. Zeltinger, and J. Kohn, "Viscoelastic properties of fibrinogen adsorbed to the surface of biomaterials used in blood-contacting medical devices", Langmuir, Vol. 23(6), pp. 3298–3304, https://doi.org/10.1021/la060500r, (2007)

[18] O. H. Campanella, H. Sumali, B. Mert and B. Patel, "The use of vibration principles to characterize the mechanical properties of biomaterials", in Biomaterials - Physics and Chemistry, Ed: R. Pignatello, InTech, https://doi.org/10.5772/22858, (2011)

[19] O. H. Campanella, H. Sumali, B. Mert and B. Patel, "The use of vibration principles to characterize the mechanical properties of biomaterials", in Biomaterials - Physics and Chemistry, Ed: R. Pignatello, InTech, https://doi.org/10.5772/22858, (2011)

[20] R. C. de Guzman, M. R. Merrill, J. R. Richter, R. I. Hamzi, O. K. Greengauz-Roberts, and M. E. Van Dyke, "Mechanical and biological properties of keratose biomaterials", Biomaterials, Vol. 32(32), pp. 8205–8217, https://doi.org/10.1016/j.biomaterials.2011.07.054, (2011)

[21] J. H. He, "Homotopy perturbation method: A new nonlinear analytical technique", Applied Mathematics and Computation, Vol. 135(1), pp. 73–79, https://doi.org/10.1016/S0096-3003(01)00312-5, (2003)

[22] T. Öziş and A. Yildirim, "Comparison between Adomian's method and He's homotopy perturbation method", Computers & Mathematics with Applications, Vol. 56(5), pp. 1216–1224, https://doi.org/10.1016/j.camwa.2008.02.023, (2008)

[23] D. H. Shou, "The homotopy perturbation method for nonlinear oscillators", Computers & Mathematics with Applications, Vol. 58(11–12), pp. 2456–2459, https://doi.org/10.1016/j.camwa.2009.03.034, (2009)

[24] H. A. Zedan and E. El Adrous, "The application of the homotopy perturbation method and the homotopy analysis method to the generalized Zakharov equations", Abstract and Applied Analysis, Vol. 2012(1), p. 561252, https://doi.org/10.1155/2012/561252, (2012)

[25] S. Saedodin and M. Shahbabaei, "Thermal analysis of natural convection in porous fins with homotopy perturbation method (HPM)", Arabian Journal for Science and Engineering, Vol. 38(8), pp. 2227–2231, https://doi.org/10.1007/s13369-013-0581-6, (2013)

[26] J. Biazar and H. Ghazvini, "Homotopy perturbation method for solving hyperbolic partial differential equations", Computers & Mathematics with Applications, Vol. 56(2), pp. 453–458, https://doi.org/10.1016/j.camwa.2007.10.032, (2008)

[27] H. A. Hoshyar, I. Rahimipetroudi, D. D. Ganji, and A. R. Majidian. "Thermal performance of porous fins with temperature-dependent heat generation via the homotopy perturbation method and collocation method." Journal of Applied Mathematics and Computational Mechanics, Vol. 14(4), pp. 53–65. https://doi.org/10.17512/jamcm.2015.4.06, (2015)

[28] R. Tripathi and H. K. Mishra, "Homotopy perturbation method with Laplace transform (LT-HPM) for solving Lane–Emden type differential equations (LETDEs)", SpringerPlus, Vol. 5(1), pp. 1–21, https://doi.org/10.1186/s40064-016-3487-4, (2016)

[29] O. Adeleye and A. Yinusa, "Heat transfer analysis of non-Newtonian natural convective fluid flow using homotopy perturbation and Daftardar-Gejiji & Jafari methods", Journal of Applied Mathematics and Computational Mechanics, Vol. 18(2), pp. 5–18, https://doi.org/10.17512/jamcm.2019.2.01, (2019)